

SUPPORTING INFORMATION

Pixelated full-colour small molecule semiconductor devices towards artificial retinas

M. Skhunov^{1*}, A.N. Solodukhin², P. Giannakou¹, L. Askew¹, Yu. N. Luponosov²,
D.O. Balakirev², N.K. Kalinichenko², I. P. Marko³, S.J. Sweeney³, S.A. Ponomarenko^{2**}

¹ Electrical and Electronic Engineering, Advanced Technology Institute, University of Surrey, Guildford, UK

² Enikolopov Institute of Synthetic Polymeric Materials of the Russian Academy of Sciences, Profsoyuznaya st. 70, Moscow 117393, Russian

³ Advanced Technology Institute and Department of Physics University of Surrey, Guildford, GU2 7XH, UK

* e-mail: m.shkunov@surrey.ac.uk

** e-mail: ponomarenko@ispm.ru

CONTENTS

1. Materials	2
2. Synthesis	2
3. ¹H and ¹³C NMR spectra	4
4. Instruments and measurements	7
5. Optical absorption (UV-VIS spectrometry)	9
6. Samples for photo-response measurements in electrolyte	10
7. Photo-response measurements in electrolyte	10
8. Inkjet Printing	11
8.1. Characterisation: optical microscopy	15
8.2. Scanning electron microscopy (SEM)	16
8.3. X-ray diffraction data	17
9. Photo-excitation measurements	17
9.1 Photo-current measurements of ink-jet printed / pixelated devices	17
9.2 Photovoltage spectra	18
10. Density functional theory (DFT) data	19
11. Electron and hole mobilities of the materials	21
12. Photo current transients for pulsed excitation	22
References	23

1. Materials

n-Butyllithium solution, 1.6 M in hexanes (*n*-BuLi), 2-ethylhexyl cyanoacetate and 3-ethylrhodanine were obtained from Sigma-Aldrich Co. and used without further purification. THF, pyridine and *N,N*-dimethylformamide (DMF) were dried and purified according to the known techniques. Diphenyl[4-(2-thienyl)phenyl]amine (**1**) was obtained as described in previous work.¹ 5,5',5''-[Nitrilotris(4,1-phenylene)]trithiophene-2-carbaldehyde (**2**) was obtained as described in previous work.² 7-[4-(diphenylamino)phenyl]-2,1,3-benzothiadiazole-4-carbaldehyde (**3**) was obtained as described in previous work.³ 2,2',2''-[nitrilotris(4,1-phenylene-2,2'-bithiene-5',5'-diylhept-1-yl-1-ylidene)]trimalononitrile **N(Ph-2T-DCV-Hex)₃** was obtained as described in previous work.⁴ All reactions, unless stated otherwise, were carried out under an inert atmosphere. PEDOT:PSS Al 4083 was purchased from Ossila and used as received.

2. Synthesis

The synthetic route to the preparation of **TPA-T-C(O)H**, **N(Ph-T-CNA-EtHex)₃** and **TPA-BTZ-Rh-Et** is shown below (Fig. S1).

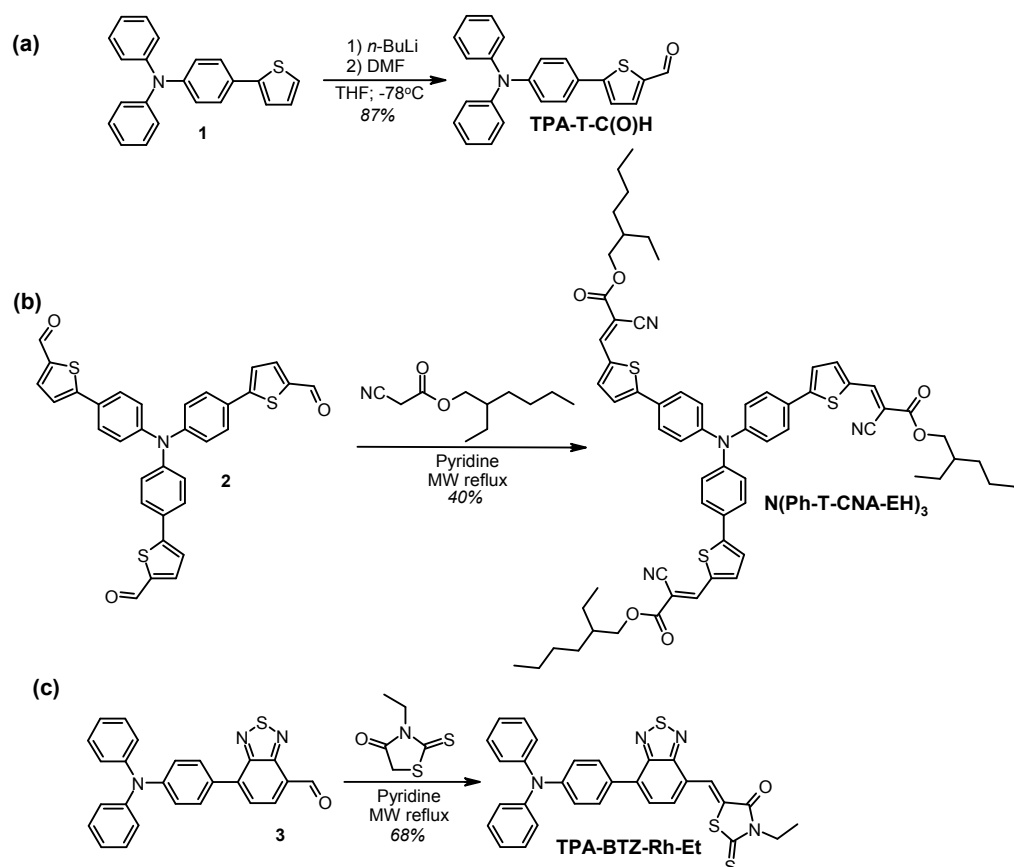


Figure S1. Synthetic scheme of **TPA-T-C(O)H** (a), **N(Ph-T-CNA-EtHex)₃** (b), **TPA-BTZ-Rh-Et** (c).

5-[4-(diphenylamino)phenyl]thiophene-2-carbaldehyde (TPA-T-C(O)H). 1.6 M solution of *n*-butyllithium (10.36 mL, 16.6 mmol) in hexane was added dropwise to a solution of compound **1** (5.43 g, 16.6 mmol) in 160 mL of dry THF at -78°C. Afterwards the reaction mixture was stirred for 60 min at -78°C and then dimethylformamide (1.22 g, 16.7 mmol) was added in one portion. The reaction mixture was stirred for 30 min at -78 °C, then the cooling bath was removed, and the stirring was continued for another 30 min with raising the temperature to RT. After reaction completion, 300 mL of diethyl ether, 100 mL of water and 17 mL of 1 M HCl were added to the reaction mixture. The combined organic phases were dried over sodium sulfate, filtered and evaporated under vacuum. The crude product was purified by column chromatography on silica gel using dichloromethane as an eluent followed by recrystallization from dichloromethane/ethanol mixture to give **TPA-T-C(O)H** (5.13 g, 87%) as a yellow solid. M.p. = 115°C. ¹H NMR (250 MHz, CDCl₃): (ppm) 7.02–7.18 (overlapping peaks, 8H); 7.25–7.34 (overlapping peaks, 5H); 7.51 (d, 2H, *J* = 8.55 Hz); 7.70 (d, 1H, *J* = 3.96 Hz); 9.85 (s, 1H). ¹³C NMR (75 MHz, CDCl₃): 122.32; 122.83; 123.84; 125.14; 126.08; 127.21; 129.46; 137.74; 141.26; 146.93; 149.10; 154.55; 182.60. Calcd (%) for C₂₃H₁₇NOS: C, 77.72; H, 4.82; N, 3.94; S, 9.02. Found C, 77.61; H, 4.77; N, 3.90; S, 8.98.

Tris(2-ethylhexyl)(2E,2'E,2''E)-3,3',3''-[nitrilotris(4,1-phenylenethiene-5,2-diyl)]tris(2-cyanoacrylate) (N(Ph-T-CNA-EtHex)₃). Compound **2** (0.93 g, 1.6 mmol), 2-ethylhexyl cyanoacetate (1.43 g, 7.3 mmol) and dry pyridine (28 mL) were placed in a reaction vessel and stirred under an argon atmosphere for 6 hours at reflux temperature using the microwave heating. After reaction was completed, pyridine was evaporated under vacuum and the residue solid was dried. The crude product was purified by column chromatography on silica gel using dichloromethane as an eluent followed by recrystallization from toluene/hexane mixture to give **N(Ph-T-CNA-EtHex)₃** (0.72 g, 40%) as a black solid. M.p. = 148°C. ¹H NMR (250 MHz, CDCl₃): 0.85–1.00 (overlapping peaks, 18H); 1.22–1.53 (overlapping peaks, 24H); 1.70 (m, *m* = 5, 3H, *J* = 6.10 Hz); 4.21 (d, 6H, *J* = 5.49 Hz); 7.18 (d, 6H, *J* = 8.85 Hz); 7.37 (d, 3H, *J* = 4.27 Hz); 7.63 (d, 6H, *J* = 8.55 Hz); 7.74 (d, 3H, *J* = 3.97 Hz); 8.27 (s, 3H). ¹³C NMR (75 MHz, CDCl₃): 10.98; 14.02; 22.91; 23.71; 28.87; 30.26; 38.73; 68.74; 97.71; 115.94; 123.85; 124.63; 127.72; 128.18; 134.58; 139.21; 146.30; 147.49; 153.83; 163.15. Calcd (%) for C₆₆H₇₂N₄O₆S₃: C, 71.19; H, 6.52; N, 5.03; S, 8.64. Found C, 71.31; H, 6.65; N, 5.00; S, 8.60.

(5Z)-5-({7-[4-(diphenylamino)phenyl]-2,1,3-benzothiadiazol-4-yl}methylene)-3-ethyl-2-thioxo-1,3-thiazolidin-4-one (TPA-BTZ-Rh-Et). Compound **3** (0.54 g, 1.3 mmol), 3-ethylrhodanine (0.32 g, 2.0 mmol) and dry pyridine (13 mL) were placed in a reaction vessel and stirred under an argon atmosphere for 8 hours at reflux temperature using the microwave

heating. After reaction was completed, pyridine was evaporated under vacuum and the residue solid was dried. The crude product was purified by column chromatography on silica gel using dichloromethane as an eluent followed by recrystallization from toluene/hexane mixture to give **TPA-BTZ-Rh-Et** (0.49 g, 68%) as a black solid. M.p. = 209°C. ¹H NMR (250 MHz, CDCl₃): 1.32 (t, 3H, *J* = 7.15 Hz); 4.23 (dd, 2H, *J*₁ = 7.15 Hz, *J*₂ = 14.30 Hz); 7.09 (t, 2H, *J* = 7.26 Hz); 7.15–7.22 (overlapping peaks, 6H); 7.26–7.34 (overlapping peaks, 4H); 7.74 (dd, 2H, *J*₁ = 7.60 Hz, *J*₂ = 16.95 Hz); 7.90 (d, 2H, *J* = 8.80 Hz); 8.50 (s, 1H). ¹³C NMR (75 MHz, CDCl₃): 12.30; 39.89; 122.04; 123.81; 124.85; 124.92; 125.29; 126.51; 127.34; 129.34; 129.45; 130.17; 131.20; 136.04; 147.06; 148.94; 153.23; 154.60; 167.46; 193.12. Calcd (%) for C₃₀H₂₂N₄OS₃: C, 65.43; H, 4.03; N, 10.17; S, 17.47. Found C, 65.66; H, 4.15; N, 10.15; S, 17.40. MALDI-MS: found *m/z* 550.10; calculated for [M]⁺ 550.10.

3. ¹H and ¹³C NMR spectra

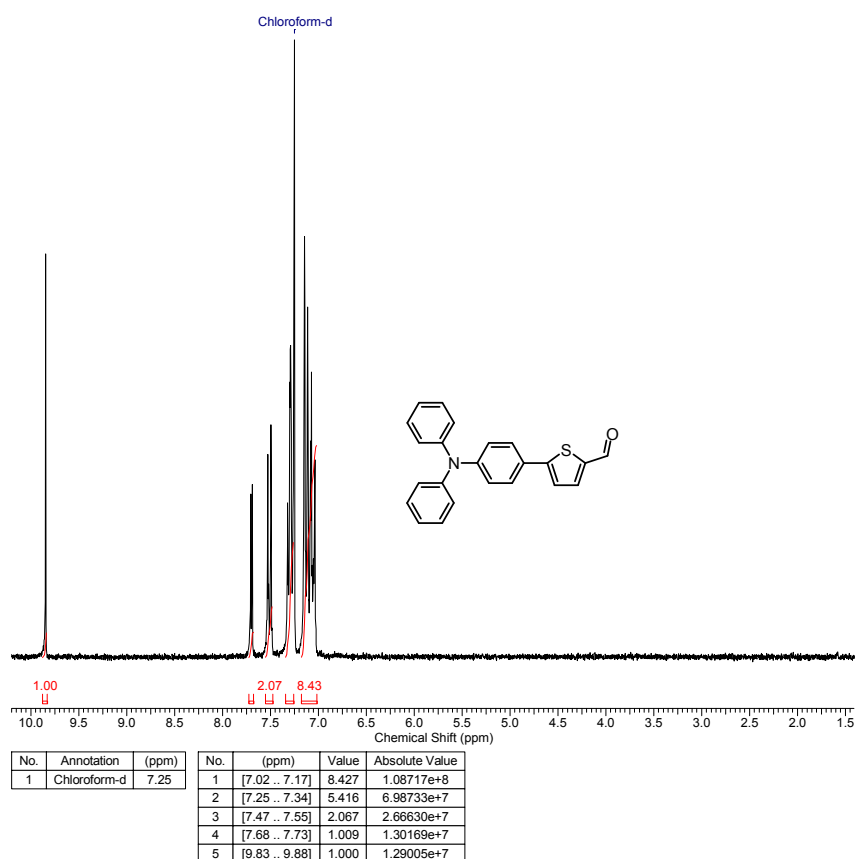


Figure S2. ¹H NMR spectra for **TPA-T-C(O)H**.

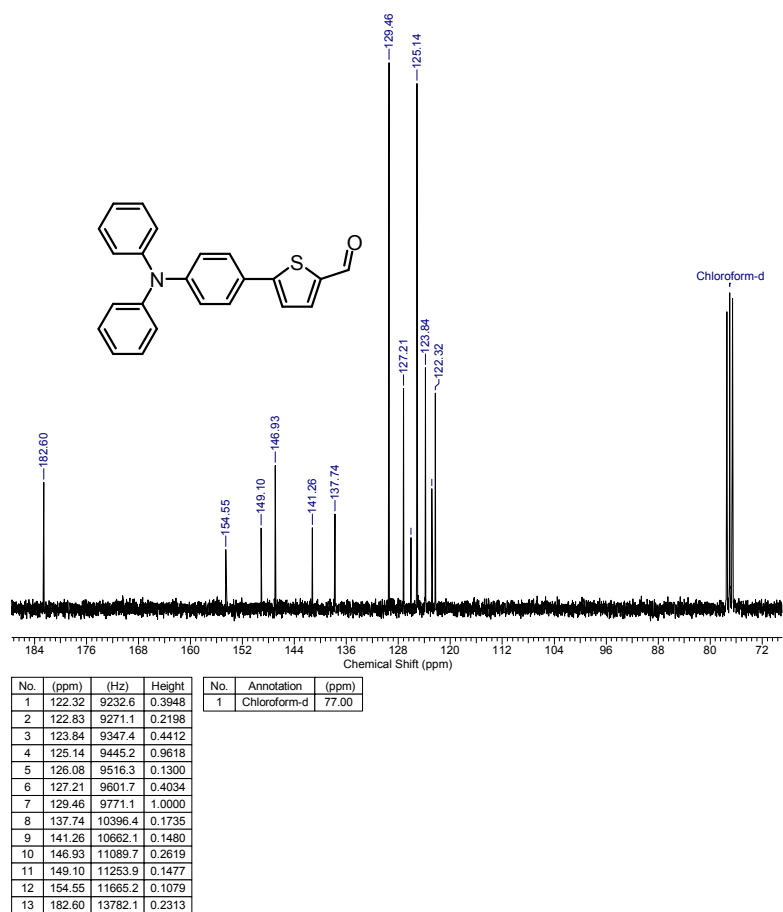


Figure S3. ^{13}C NMR spectra for TPA-T-C(O)H.

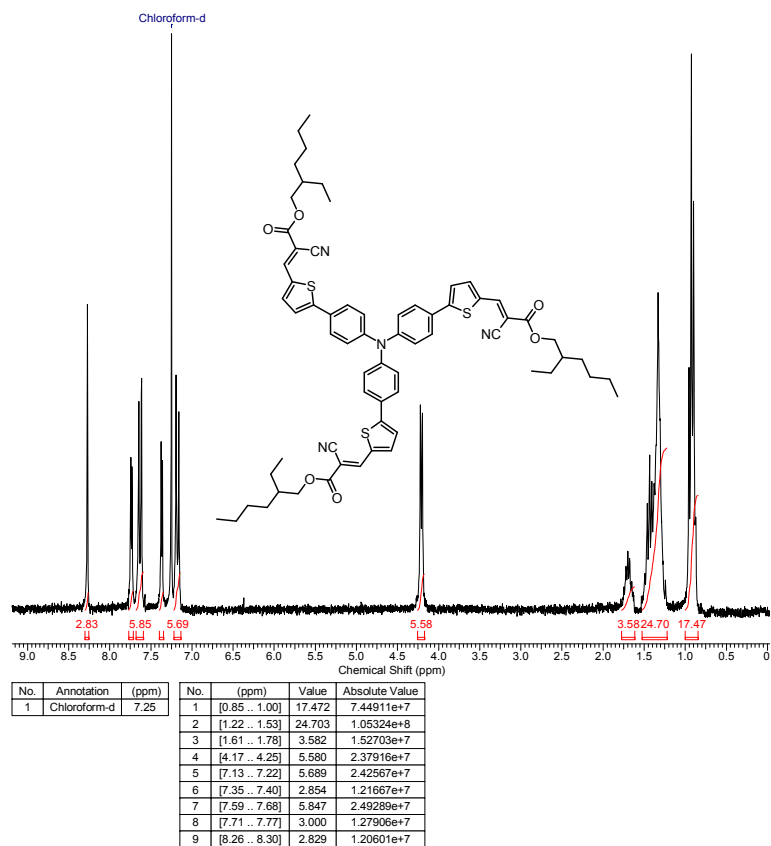


Figure S4. ^1H NMR spectra for N(Ph-T-CNA-EtHex)₃.

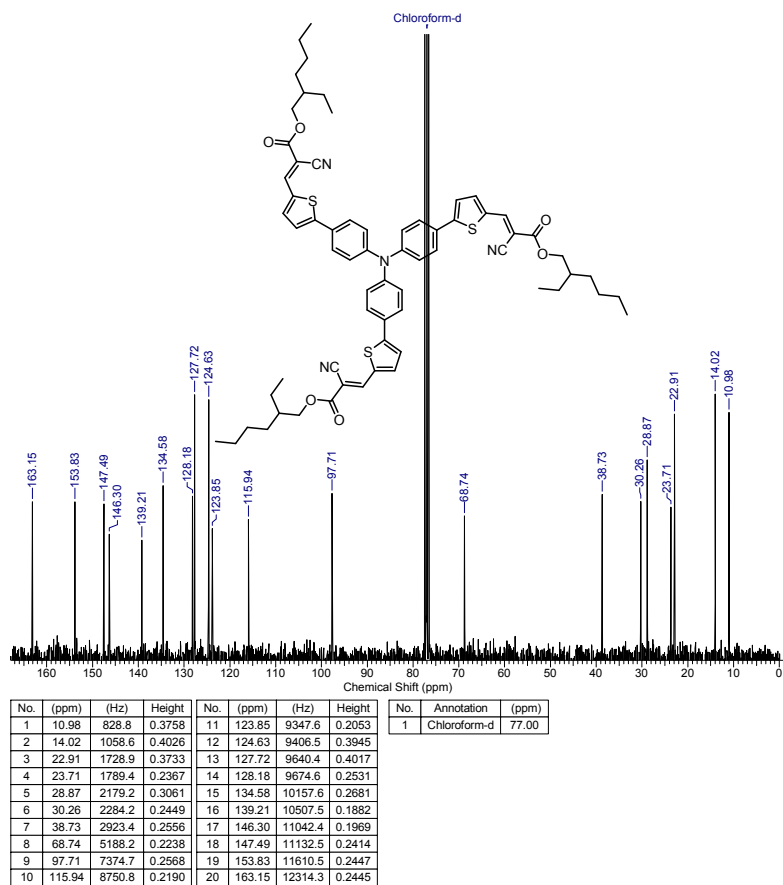


Figure S5. ^{13}C NMR spectra for $\text{N}(\text{Ph-T-CNA-EtHex})_3$.

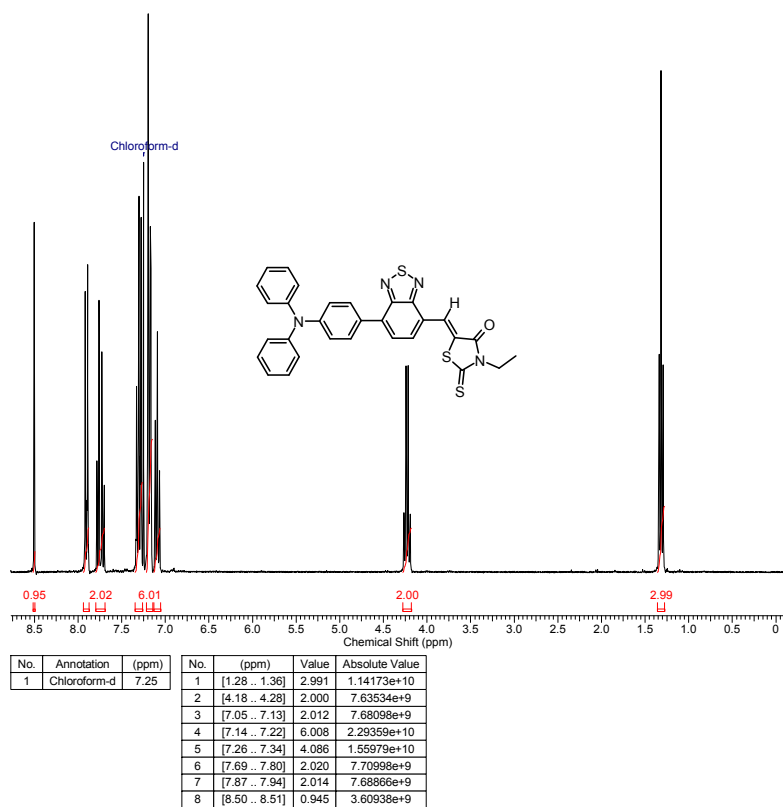


Figure S6. ^1H NMR spectra for TPA-BTZ-Rh-Et .

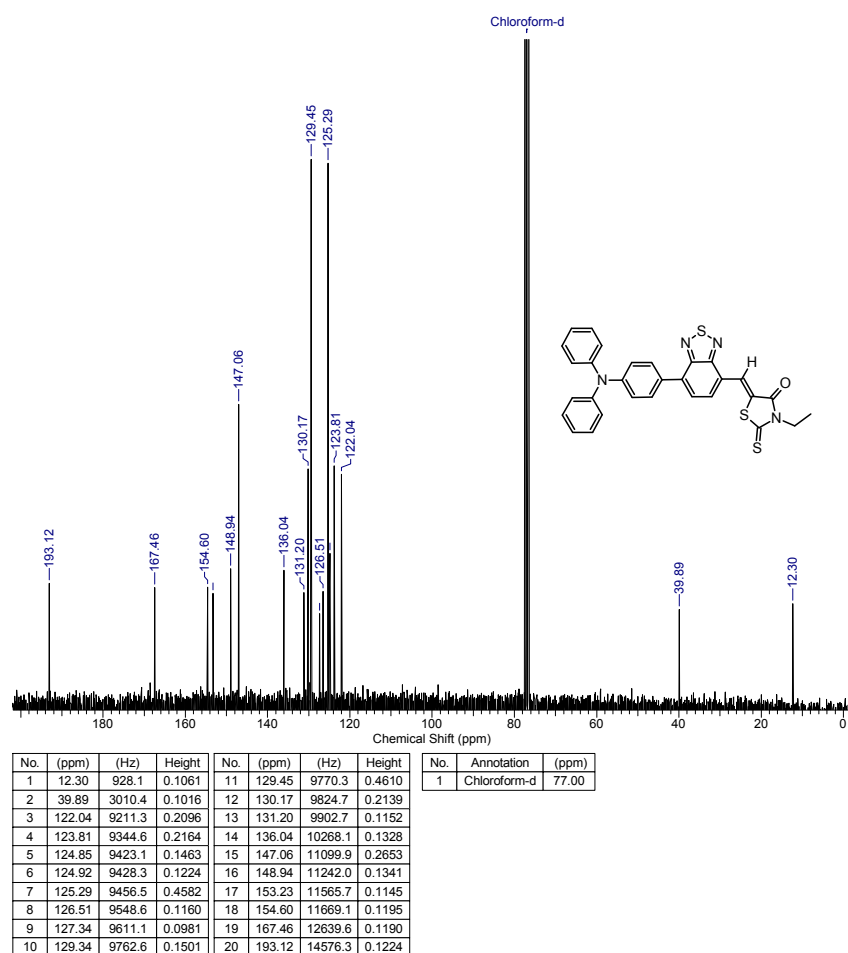


Figure S7. ^{13}C NMR spectra for TPA-BTZ-Rh-Et.

4. Instruments and measurements

^1H NMR spectra were recorded in a “Bruker WP-250 SY” spectrometer, working at a frequency of 250.13 MHz and using CDCl_3 signal (7.25 ppm) as the internal standard. ^{13}C NMR spectra were recorded using a “Bruker Avance II 300” spectrometer at 75 MHz. In the case of ^1H NMR spectroscopy, the compounds to be analysed were taken in the form of 1% solutions in CDCl_3 . In the case of ^{13}C NMR spectroscopy, the compounds to be analysed were taken in the form of 5% solutions in CDCl_3 . The spectra were then processed on the computer using the ACD Labs software.

Mass-spectra (MALDI) were registered on the Autoflex II Bruker (resolution FWHM 18000), equipped with a nitrogen laser (emission wavelength 337 nm) and time-of-flight mass-detector working in reflections mode. The accelerating voltage was 20 kV. Samples were applied to a polished stainless steel substrate. Spectrum was recorded in the positive ion mode. The resulting spectrum was the sum of 300 spectra obtained at different points of sample. 2,5-Dihydroxybenzoic acid (DHB) (Acros, 99%) and α -cyano-4-hydroxycinnamic acid (HCCA) (Acros, 99%) were used as matrices.

Elemental analysis of C, N and H elements was carried out using CHN automatic analyzer CE 1106 (Italy). The settling titration using BaCl₂ was applied to analyze sulphur. Experimental error for elemental analysis is 0.30–0.50%. In the case of column chromatography, silica gel 60 (“Merck”) was taken.

The Knövenagel condensation was carried out in the microwave “Discovery”, (CEM corporation, USA), using a standard method with the open vessel option, 30 watts.

Cyclic voltammetry measurements were carried out using solid compact layers of the oligomers, which in turn were made by electrostatically rubbing the materials onto a glassy carbon electrode using IPC-Pro M potentiostat. Measurements were made in acetonitrile solution using 0.1 M Bu₄NPF₆ as supporting electrolyte. The scan rate was 200 mV s⁻¹. The glassy carbon electrode was used as a work electrode. Potentials were measured relative to a saturated calomel electrode (SCE). The highest occupied molecular orbital (HOMO) and the lowest unoccupied molecular orbital (LUMO) energy levels were calculated using the first standard formal oxidation and reduction potentials obtained from CV experiments in films according to following equation: LUMO = e(φ_{red}+4.40)(eV) and HOMO = -e(φ_{ox}+4.40)(eV).⁵

Absorption profiles were recorded with a multifunctional spectrometer ALS01M. Films were cast from THF, chlorobenzene, *o*-dichlorobenzene or chloroform solutions on glass substrates.

XRD measurements were carried out at Rigaku SmartLab diffractometer with rotating Cu-anode. The incident beam was formed with multilayer parabolic mirror that provide “pink” (Cu Kα, wavelength 1.54056 Å) X-ray beam with angular divergence ≈0.01° in a scattering plane. X-ray diffractometry patterns were obtained by detector scans with incidence angle 0.25 degree. The slit before samples was 1 mm, slits between samples and detector – 0.5 mm, angular step and scanning speed was chosen from experimental data and SN ratio. Film thicknesses were determined from X-Ray reflectivity experiments as described in the reference.⁶

5. Optical absorption (UV-VIS spectrometry)

Optical absorption of diluted solutions were recorded with an absorption spectrometer Shimadzu UV 2501 PC at room temperature in THF solutions (10^{-5} M).

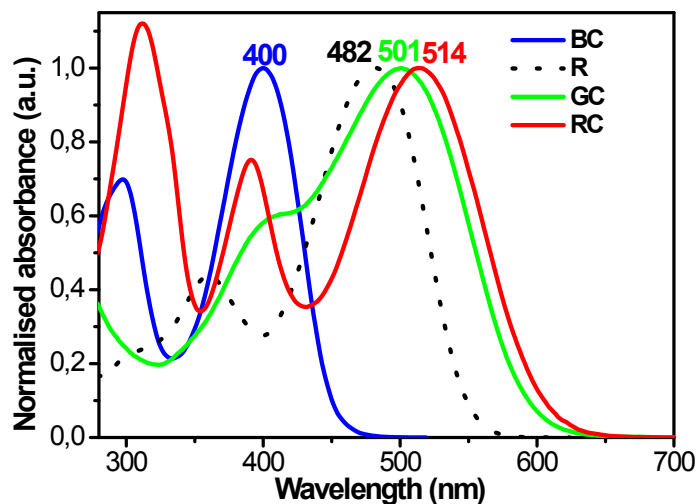


Figure S8. Absorption spectra of TPA-T-C(O)H (BC), N(Ph-T-CNA-EtHex)₃ (R), N(Ph-2T-DCV-Hex)₃ (GC), TPA-BTZ-Rh-Et (RC) in THF solution.

Thin films were prepared by spin-coating or drop-casting 5-15 mg/mL solutions of the materials in chlorobenzene or *o*-dichlorobenzene on glass and quartz substrates, and optical absorption data were collected with a Carey 5000 UV-VIS spectrophotometer.

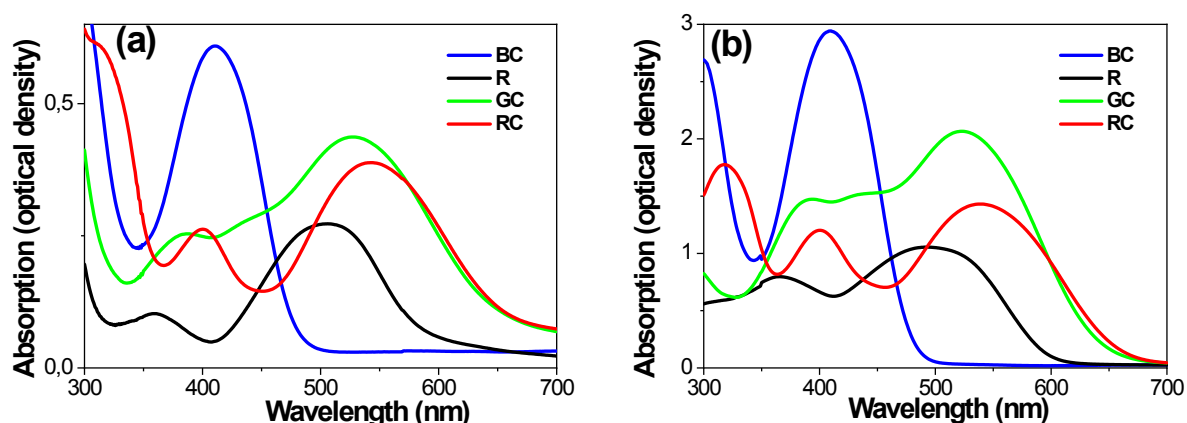


Figure S9. Absorption spectra of TPA-T-C(O)H (BC), N(Ph-T-CNA-EtHex)₃ (R), N(Ph-2T-DCV-Hex)₃ (GC), TPA-BTZ-Rh-Et (RC): (a) thin films (30 – 60nm) on glass/ITO/ZnO substrates produced by spin-coating; (b) thicker (60-90nm) films on glass/ITO substrates produced by drop casting. BC – ‘blue cones’, GC – ‘green cones’, RC – ‘red cones’, R – ‘rods’.

6. Samples for photo-response measurements in electrolyte

Device structure: glass/ITO/active layer, and glass/ITO/ZnO/active layer (Figure S10). Glass /ITO substrates (20 Ohms/square) were cleaned by sonication in DI water, acetone, isopropanol, 5 min each, and dried with nitrogen gun. Samples were then UV Ozone treated for 25 minutes to remove organic surface residues. ZnO precursor was prepared as described⁷ and spin-coated at 3500 rpm for 1 min, and then converted to ZnO on a hot plate in air at 275°C. Samples were solvent cleaned to remove the precursor residues by 3 min sonication in water, acetone and isopropanol, and dried with nitrogen gun.

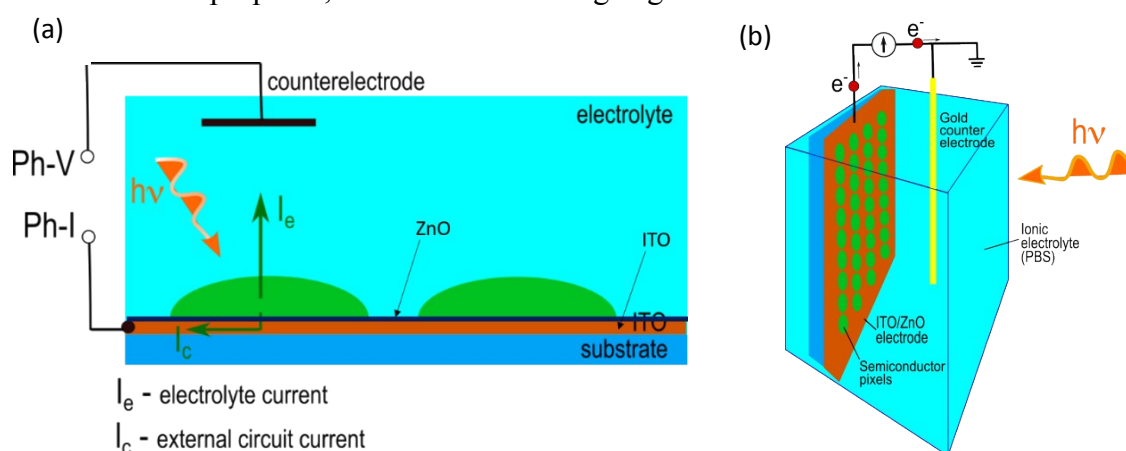


Figure S10. (a) Cross section schematic of the device structure showing position of ZnO layer; (b) schematic of electrolyte filled cell with printed pixelated sample.

7. Photo-response measurements in electrolyte

Samples were positioned inside a plastic cuvette ($10 \times 10 \times 50 \text{ mm}^3$) filled with PBS, and electrical connection was made as shown in the diagrams (Figures S11 and S10b). The photocurrent/voltage spectra were measured over the range from 370 to 700 nm by using a Signal Recovery 7265 lock-in amplifier and a 100W Bentham quartz-halogen (QH) lamp connected to a Bentham triple-grating monochromator TMC-300. Spectrometer output line width was $\sim 3 \text{ nm}$ (FWHM). A calibrated silicon reference detector was used for spectral response correction to remove the optical system contribution from the measured photocurrent spectra. Photo-response of the sample was recorded vs excitation wavelength, whereas photovoltage or photocurrent was recorded, by changing input setting on the lock-in amplifier. Samples were normally exposed to light from the electrolyte side.

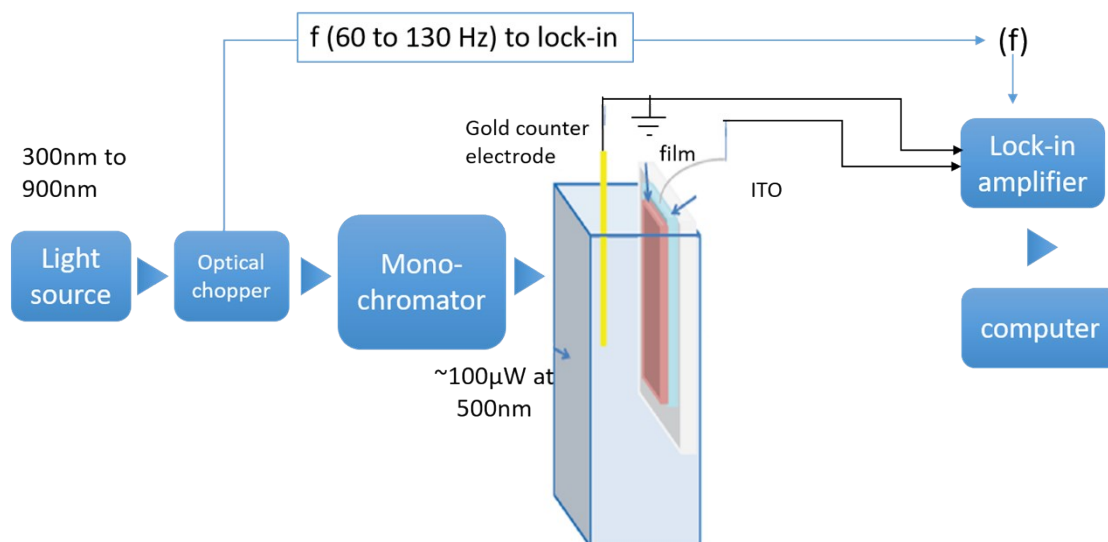


Figure S11. Schematic of photo-response measurement setup. (not to scale).

8. Inkjet Printing

Ink Preparation

The inks were prepared using **TPA-BTZ-Rh-Et**, **N(Ph-2T-DCV-Hex)₃**, **TPA-T-C(O)H** and **N(Ph-T-CNA-EtHex)₃** molecules dissolved in tetralin at 20 mg/mL concentration (red, green blue and rods respectively). All four inks were filtered using a 0.45 µm pore size PTFE syringe filter. Tetralin has viscosity of 2.02 cP at 25 °C and surface tension of 35.9±3.0 dyne/cm.⁸

Substrates Preparation

ITO glass pieces were cleaned in water, isopropanol and acetone with five minutes sonication in each solvent, and dried with compressed nitrogen gun. The substrates were then exposed to oxygen plasma (100 W for 5min) followed by deposition of ZnO precursor using spin coating (3500 rpm for 1 min) and converted to ZnO at 275 °C in air.⁷ Ultrathin polystyrene (Mw=50k) layer was deposited on the ZnO layer using spin coating (1mg/mL in toluene, 6500 rpm for 1 min). Polystyrene was used to isolate bare ITO (and ITO/ZnO) surface in pixelated samples from the interaction with electrolyte. Second function of thin (20nm) polystyrene layer is to constrain the spread of the individual droplets and to achieve smaller pixels. During jetting, upon making contact with the substrate, ink droplet, with 98%wt of tetralin, dissolves the polystyrene layer and active material is coming into the contact with the ITO, or ZnO in ITO/ZnO samples.

Printed samples were produced on the following substrates: glass/ITO, glass/ITO/PS, glass/ITO/ZnO, glass/ITO/ZnO/PS.

Printing Process

For the printing process, a Dimatix Materials (DMP 2800) Drop-On-Demand piezoelectric printer (Dimatix-Fujifilm Inc.) was used with 1 pL cartridges (DMC-11601) except the blue ink (TPA-T-C(O)H) where a 10 pL cartridge was used (DMC-11610). The temperature of the printheads was set at 30°C. The waveform and piezoelectric voltage were set to form a stable droplet formation and a droplet jetting velocity of 4 - 5 m/s. The jetting frequency was set at 2.0 kHz for all the inks. Piezo driver voltage was adjusted for each ink to achieve as minimum volume material ejection as possible (within the stable droplet formation limits), as observed by the on-board strobe camera. We note that the actual ejected droplet volume is dependent on the type of cartridge used (1pL or 10pL), piezo voltage settings, waveform and ink rheological properties.

Dimatix Materials Printer DMP 2800 can jet inks with the viscosity range of 2 – 30 cps and surface tension of about 28 – 30 dynes/cm. Tetralin has viscosity of 2.02 cP and surface tension of 35.9±3.0 dyne/cm at 25 °C. In these experiments, the temperature of the ink cartridge was set at 30°C to lower the surface tension of the ink. In some cases, low viscosity of tetralin made the inks prone to jetting instabilities; hence the formation of some non-circular pixels. Significantly larger droplet diameter for TPA-T-C(O)H (Blue) ink was obtained due to larger droplet volume related to the corresponding cartridge (10 pL DMC-11610).

Even though the materials printed on polystyrene layer showed slight improvement in size, for **TPA-T-C(O)H** (Blue) the droplet size on plain substrates (ZnO) was ~30 μm whereas on polystyrene-coated substrate was 70 μm. It is believed that this has to do with the way that droplets evaporate. In polystyrene-coated substrate the size of the droplet is the same as the droplet's footprint upon impact with the substrate. However, on plain substrates (ITO, and ITO/ZnO), the droplet evaporates to the edges (no droplet pinning takes place) concentrating the solute to the centre (Marangoni flow), causing the edge line to contract to a new width with smaller footprint area. This 'slip-stick' pattern is similar to those that have been previously reported for self-assembly studies using dip coating⁸

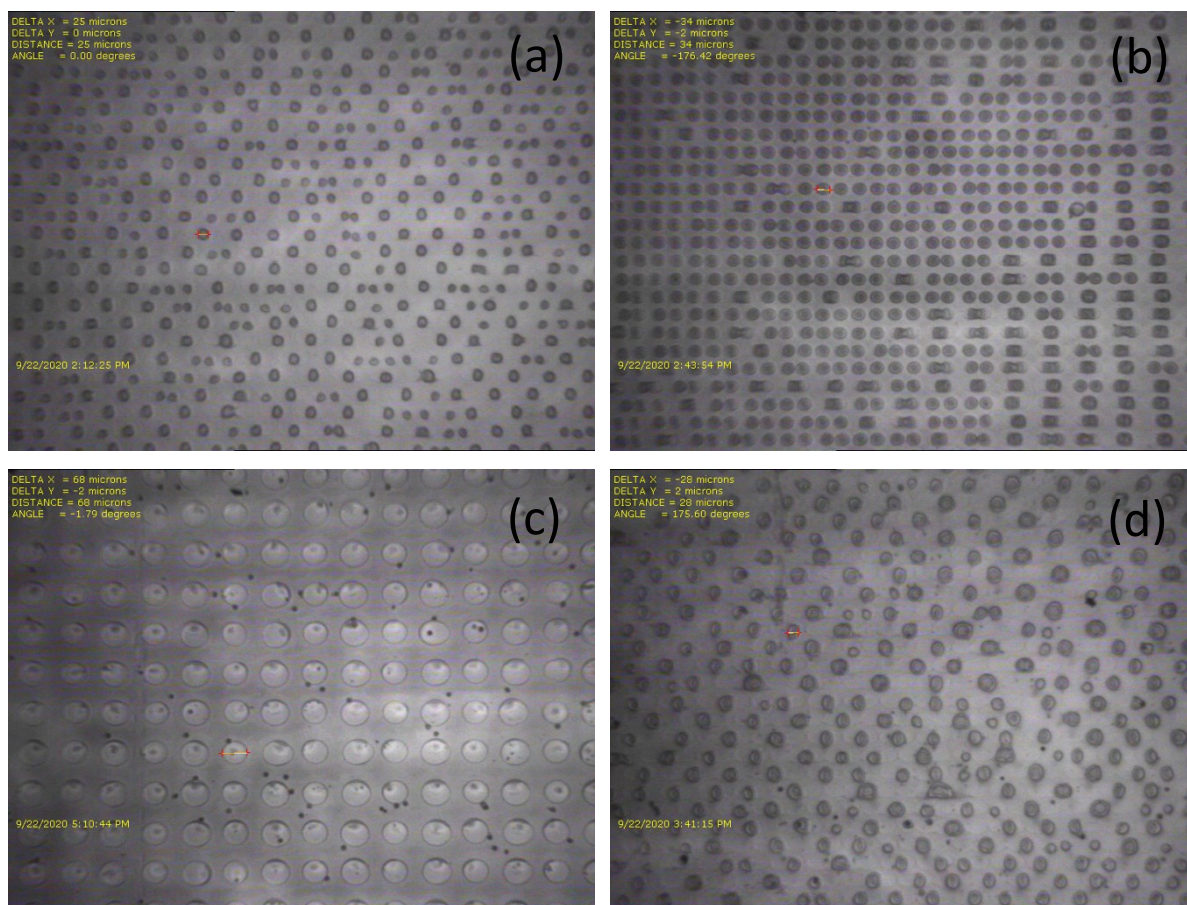


Figure S12. Fiducial images of inkjet-printed (a) **TPA-BTZ-Rh-Et** (RC) (Red) (b) **N(Ph-2T-DCV-Hex)₃** (GC) (Green) (c) **TPA-T-C(O)H** (BC), (Blue) and (d) **N(Ph-T-CNA-EtHex)₃** (R) (Rods) inks on polystyrene layer.

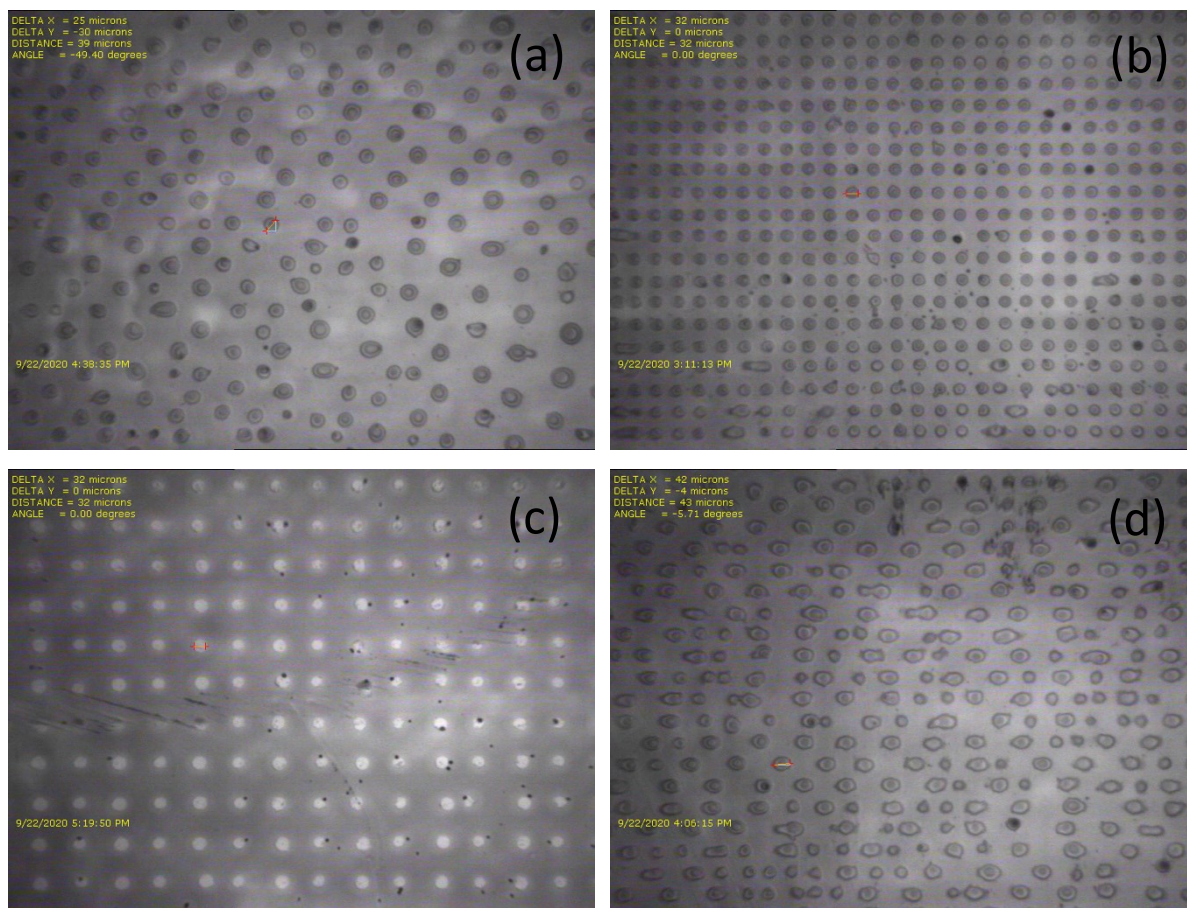


Figure S13. Fiducial images of inkjet-printed (a) TPA-BTZ-Rh-Et (RC) (Red) (b) N(Ph-2T-DCV-Hex)₃ (GC) (Green) (c) TPA-T-C(O)H (BC), (Blue) and (d) N(Ph-T-CNA-EtHex)₃ (R) (Rods) on ZnO layer (no polystyrene layer).

8.1. Characterisation: optical microscopy

Optical microscopy was conducted with Leica DM2500P polarised microscope with 5x, 10x, 20x objectives with illumination from the top of the samples.

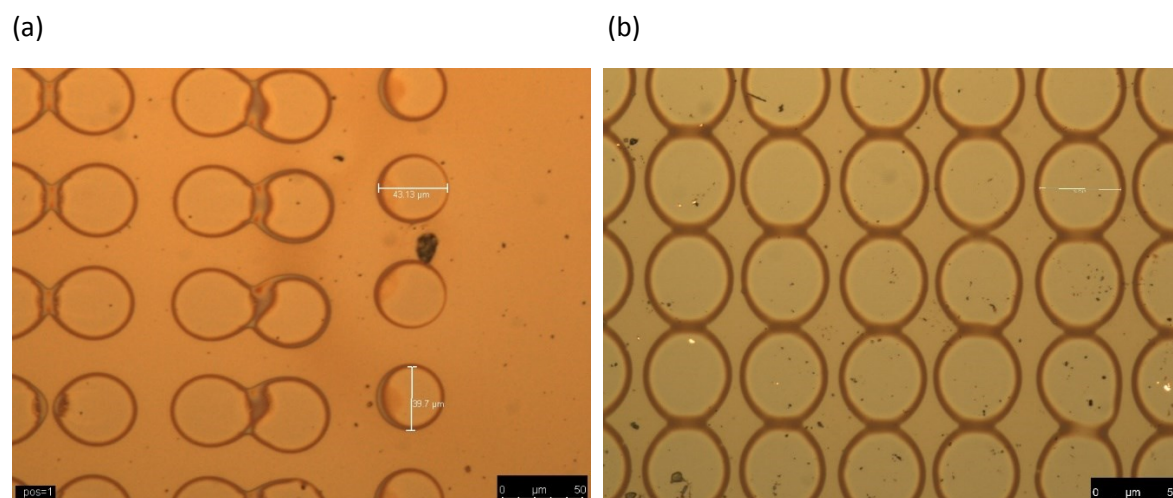


Figure S14. Optical microscope images of ink-jet printed small molecules on glass/ITO/ZnO/PS substrates: (a) TPA-BTZ-Rh-Et; (b) N(Ph-2T-DCV-Hex)₃.

8.2. Scanning electron microscopy (SEM)

SEM images were obtained with MIRA Tescan electron Microscope, operating at 5kV accelerating voltage.

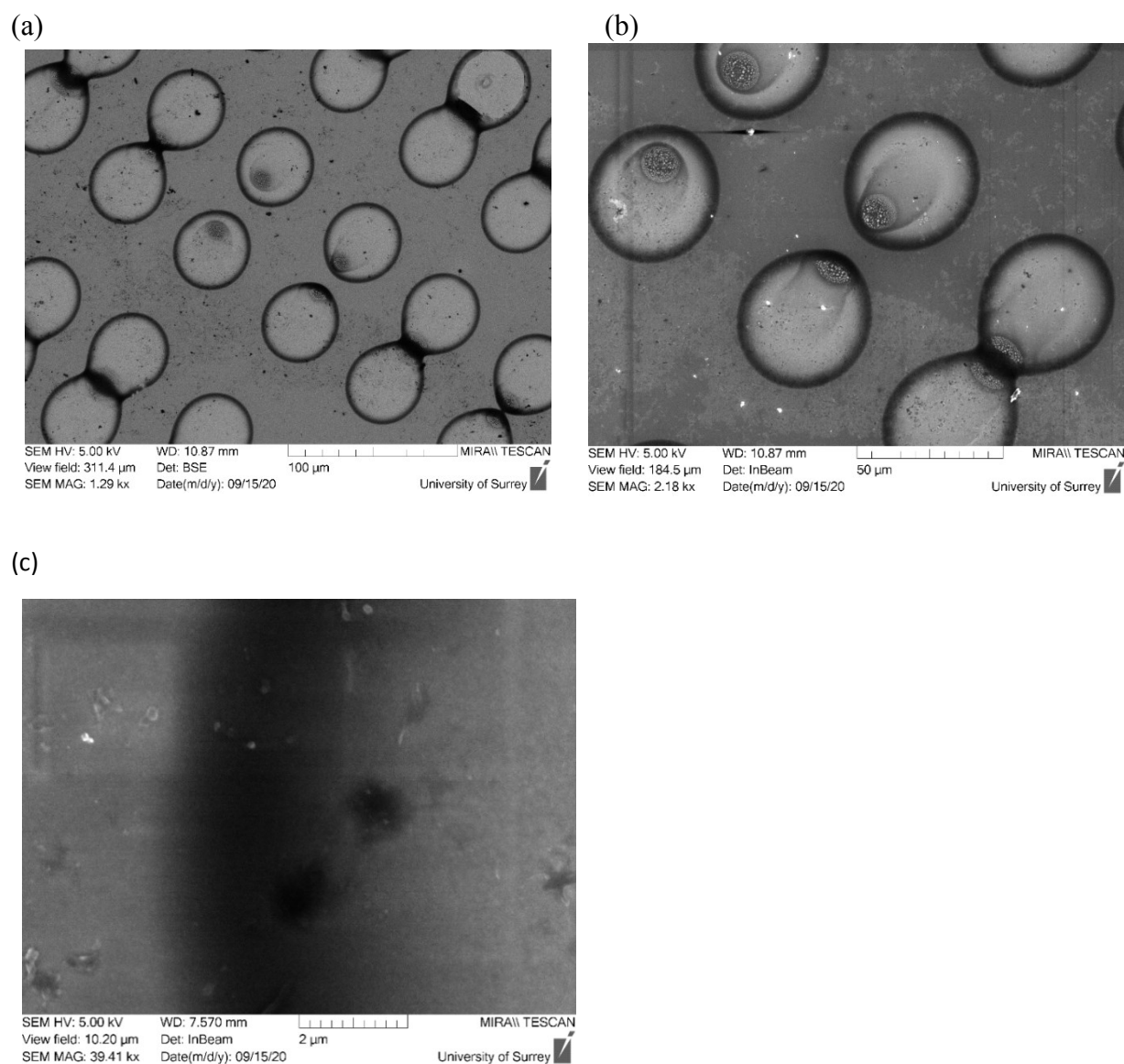


Figure S15. SEM images of ink-jet printed **TPA-BTZ-Rh-Et** sample on glass/ITO/ZnO/PS substrate. Printed with 1 pL cartridge. Various magnifications: (a) 1290x; (b) 2180x (c) pixel edge, magnification 3941x.

8.3. X-ray diffraction data

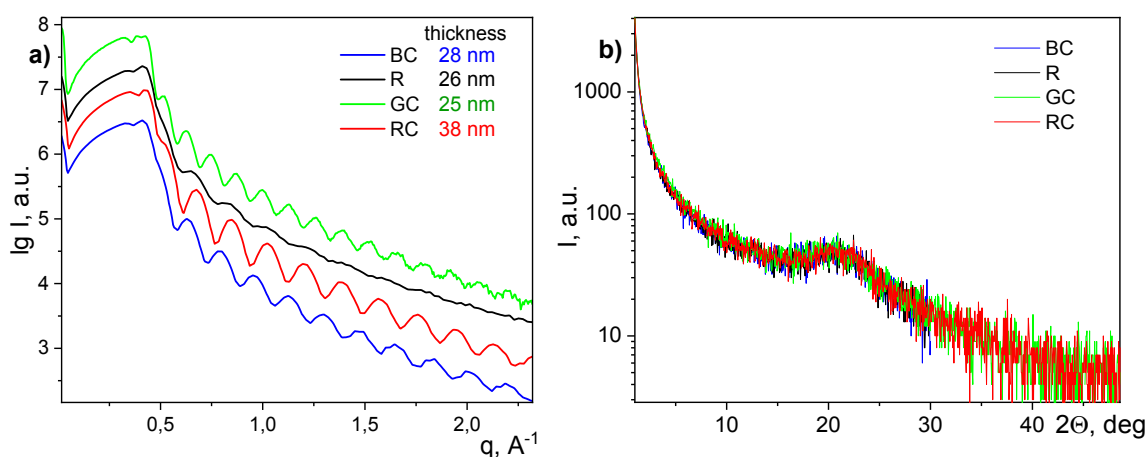


Figure S16. X-ray reflectometry curves (a), grazing incidence diffraction patterns by detector scans with incidence angle 0.25 degree (b) of TPA-T-C(O)H (BC), N(Ph-T-CNA-EtHex)₃ (R), N(Ph-2T-DCV-Hex)₃ (GC), TPA-BTZ-Rh-Et (RC) thin films (25 – 38 nm) on silicon substrates produced by drop casting. Film thicknesses were determined from X-Ray reflectivity experiments.

9. Photo-excitation measurements

9.1 Photo-current measurements of ink-jet printed / pixelated devices

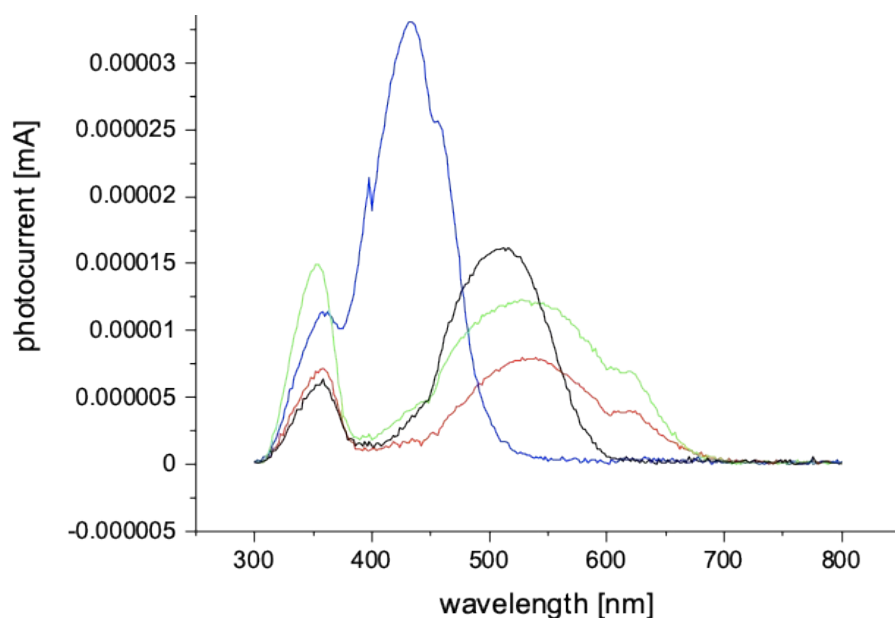
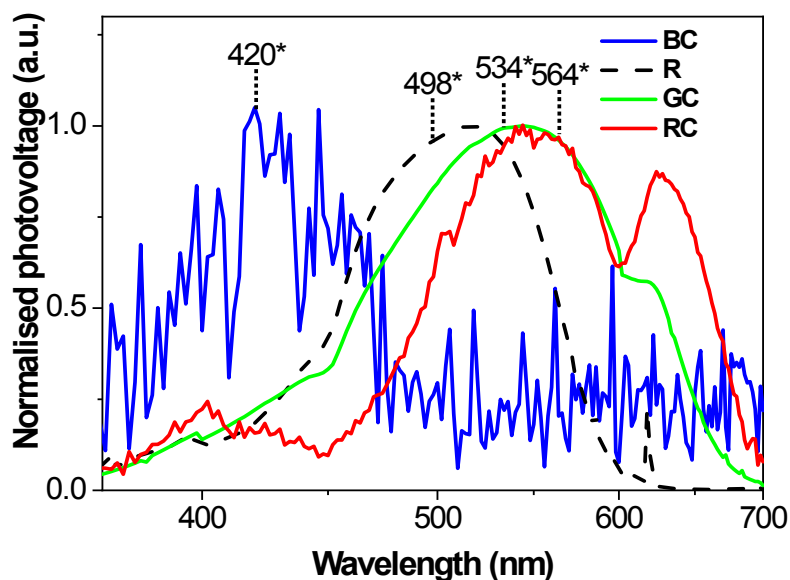


Figure S17. As-measured photocurrent spectra of ink-jet printed small molecules TPA-T-C(O)H (blue curve), N(Ph-T-CNA-EtHex)₃ (black curve), N(Ph-2T-DCV-Hex)₃ (green curve) and TPA-BTZ-Rh-Et (red curve) on glass/ITO/ZnO substrates.

9.2 Photovoltage spectra

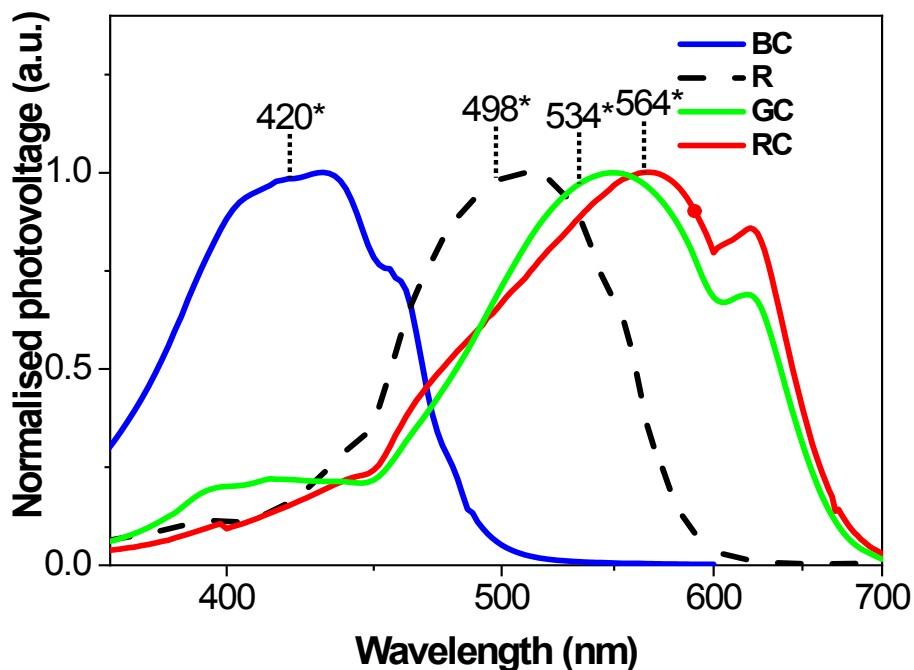


Note:* Spectral response maxima of human photoreceptors

Figure S18. Photovoltage spectra of TPA-T-C(O)H (BC), N(Ph-T-CNA-EtHex)₃ (R), N(Ph-2T-DCV-Hex)₃ (GC), TPA-BTZ-Rh-Et (RC) thicker (60-90nm) films on glass/ITO (drop casting).

Table S1. The values of the absorption maxima and photovoltage for the studied films of materials (drop casting).

Compound	Absorption maximum, nm	Voltage, mV
TPA-T-C(O)H	430	0.006
N(Ph-T-CNA-EtHex) ₃	515	1.44
N(Ph-2T-DCV-Hex) ₃	540	5.61
TPA-BTZ-Rh-Et	555	0.095



Note:* Spectral response maxima of human photoreceptors

Figure S19. Photovoltage spectra of TPA-T-C(O)H (BC), N(Ph-T-CNA-EtHex)₃ (R), N(Ph-2T-DCV-Hex)₃ (GC), TPA-BTZ-Rh-Et (RC) films on glass/ITO/ZnO (spin coating).

Table S2. The values of the absorption maxima and photovoltage for the studied films of materials (spin coating on ITO/ZnO).

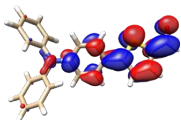
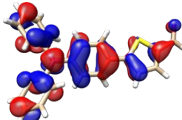
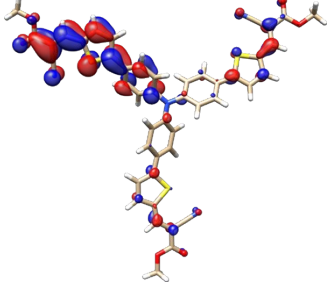
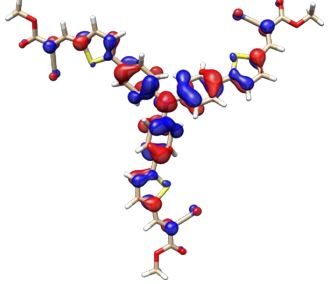
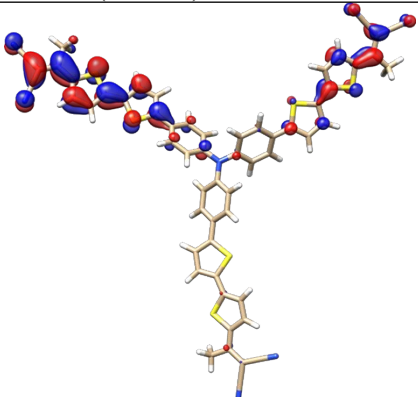
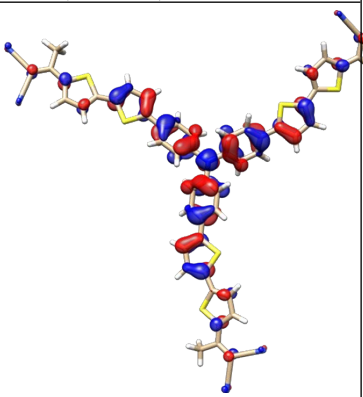
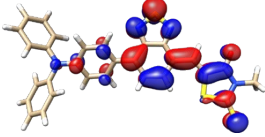
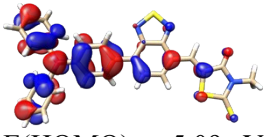
Compound	Absorption maximum, nm	Voltage, mV
TPA-T-C(O)H	431	0.055
N(Ph-T-CNA-EtHex) ₃	510	3.90
N(Ph-2T-DCV-Hex) ₃	566	1.52
TPA-BTZ-Rh-Et	549	0.03

10. Density functional theory (DFT) data

Density functional theory (DFT) calculations were performed using ORCA v. 4.0.1 software package with B3LYP5/6-31G[d] approximation. Unconstrained optimization followed by TD DFT for a ground and 15 excited states over 24 orbital vectors were applied.

Frontier orbitals are contoured at their ± 0.025 levels using Chimera v. 1.15. Nine lower TD DFT excited states presented hereafter in the spectrum together with their energy relative to the corresponding ground state.

Table S3. Frontier orbitals of the calculated conformers of **TPA-T-C(O)H**, **N(Ph-T-CNA-EtHex)₃**, **N(Ph-2T-DCV-Hex)₃** and **TPA-BTZ-Rh-Et**. To simplify the calculation the methyl radical was used instead of the hexyl one.

Molecule	Orbital	
	LUMO	HOMO
TPA-T-C(O)H $E_{tot} = -1414 E_h$; $G_0 = 3.21 \text{ eV}$	 $E(\text{LUMO}) = -1.84 \text{ eV}$	 $E(\text{HOMO}) = -5.05 \text{ eV}$
N(Ph-T-CNA-EtHex)₃ $E_{tot} = -3596 E_h$; $G_0 = 2.64 \text{ eV}$	 $E(\text{LUMO}) = -2.70 \text{ eV}$	 $E(\text{HOMO}) = -5.34 \text{ eV}$
N(Ph-2T-DCV-Hex)₃ $E_{tot} = -4962 E_h$; $G_0 = 2.33 \text{ eV}$	 $E(\text{LUMO}) = -3.03 \text{ eV}$	 $E(\text{HOMO}) = -5.36 \text{ eV}$
TPA-BTZ-Rh-Et $E_{tot} = -2604 E_h$; $G_0 = 2.19 \text{ eV}$	 $E(\text{LUMO}) = -2.90 \text{ eV}$	 $E(\text{HOMO}) = -5.09 \text{ eV}$

11. Electron and hole mobilities of the materials

Table S4. Electron and hole mobilities of the materials

Compound	Thickness [nm]	μ_h , $\text{cm}^2\text{V}^{-1}\text{s}^{-1}$	Thickness [nm]	μ_e , $\text{cm}^2\text{V}^{-1}\text{s}^{-1}$	μ_h / μ_e
BC	25 and 35	$(1.9 \pm 0.6) \cdot 10^{-5}$	54 and 63	$(5.9 \pm 0.7) \cdot 10^{-4}$	1 / 31
R	33 and 44	$(2.3 \pm 0.5) \cdot 10^{-5}$	33 and 47	$(2.5 \pm 0.9) \cdot 10^{-7}$	92 / 1
GC	42 and 74	$(1.5 \pm 0.4) \cdot 10^{-4}$	42 and 74	$(1.15 \pm 0.12) \cdot 10^{-5}$	13 / 1
RC	27 and 40	$(3.4 \pm 1.3) \cdot 10^{-5}$	30 and 60	$(3.8 \pm 0.9) \cdot 10^{-6}$	8.9 / 1

All electrical measurements were performed in a glove box with Ar atmosphere ($\text{H}_2\text{O} < 0.1$ ppm, $\text{O}_2 < 5$ ppm). Charge-carrier mobilities were determined from the space-charge-limited-current (SCLC) measurements of unipolar thin-film devices of several thicknesses.

The structure of the hole-only devices was ITO/PEDOT:PSS/N(Ph-nT-DCV-R)₃/Ag, and that of the electron-only devices was ITO/ZnO/N(Ph-nT-DCV-R)₃/Ca. In both cases, eight devices were formed on the same substrate. The hole and electron mobilities were extracted by fitting the current-voltage (J - V) characteristics of the devices with the simplest SCLC model.

According to the simplest SCLC model and taking into account the series (R_s) and shunt (R_{sh}) resistances (as fitting parameters), the charge mobility was calculated by approximating the dark J-V curves of unipolar devices using the following equation:

$$J = \frac{9}{8} \varepsilon \varepsilon_0 \mu \frac{(V - V_{BI} - JSR_s)^2}{d^3} + \frac{V - JSR_s}{R_{sh}}, \quad (\text{S1})$$

where $\varepsilon_0 = 8.85 \cdot 10^{-12}$ F/m, ε is the dielectric permittivity (taken as 3), d is the active layer thickness (measured by AFM), V_{BI} is the built-in voltage (fitting parameter).

J - V characteristics of the SMOSC were measured using a source-meter (SourceMeter 2400, Keithley) in dark and under light of a solar simulator (Newport 67005) with an intensity of 100 mW/cm² (AM1.5G).

12. Photo current transients for pulsed excitation

Measurements were conducted with pulsed low-power laser diodes, as described in section 2.4 main text.

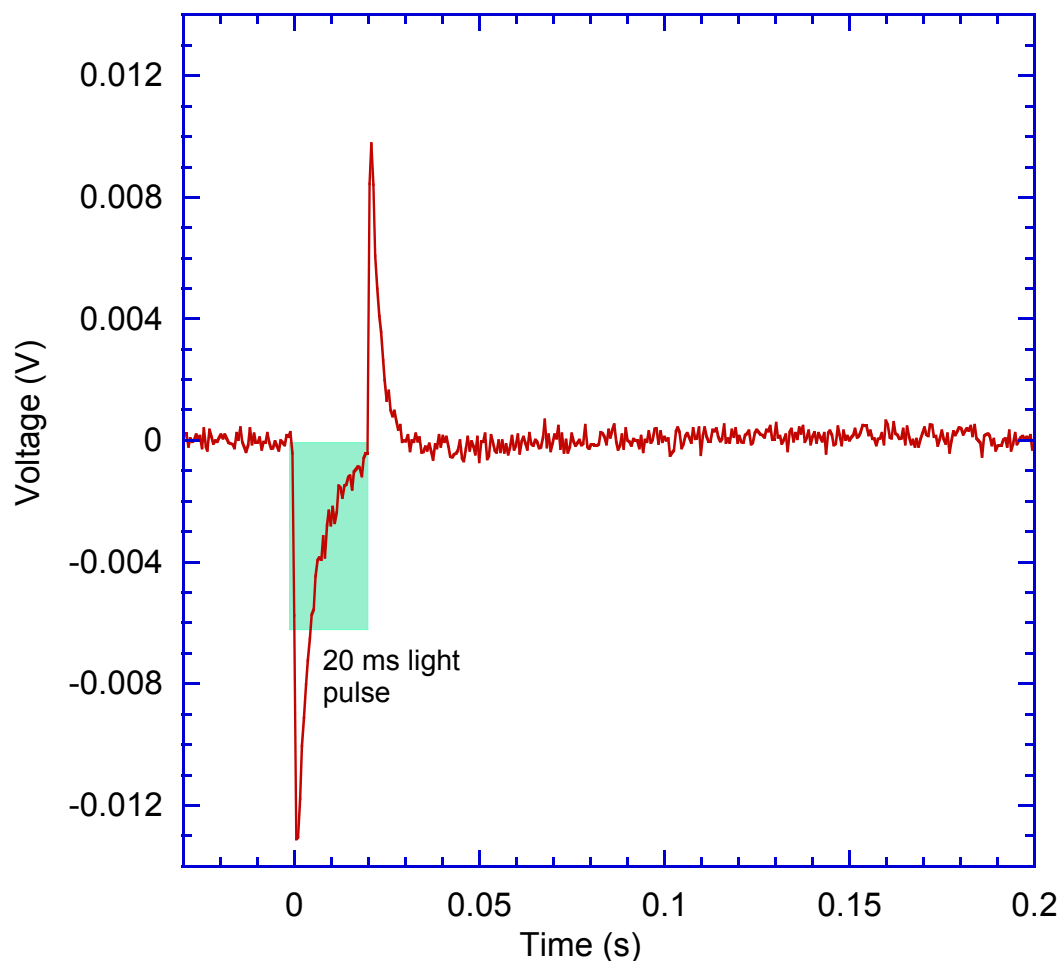


Figure S20. Transient photo-induced current response of thin film, R, $\text{N}(\text{Ph-2T-DCV-Hex})_3$ sample on glass/ITO/ZnO substrates interfaced with PBS electrolyte obtained with pulsed excitation from 515 nm laser diode. Laser pulse width 20 ms, duty cycle 999 ms. Shaded box illustrates laser pulse width. Mostly capacitive response is demonstrated.

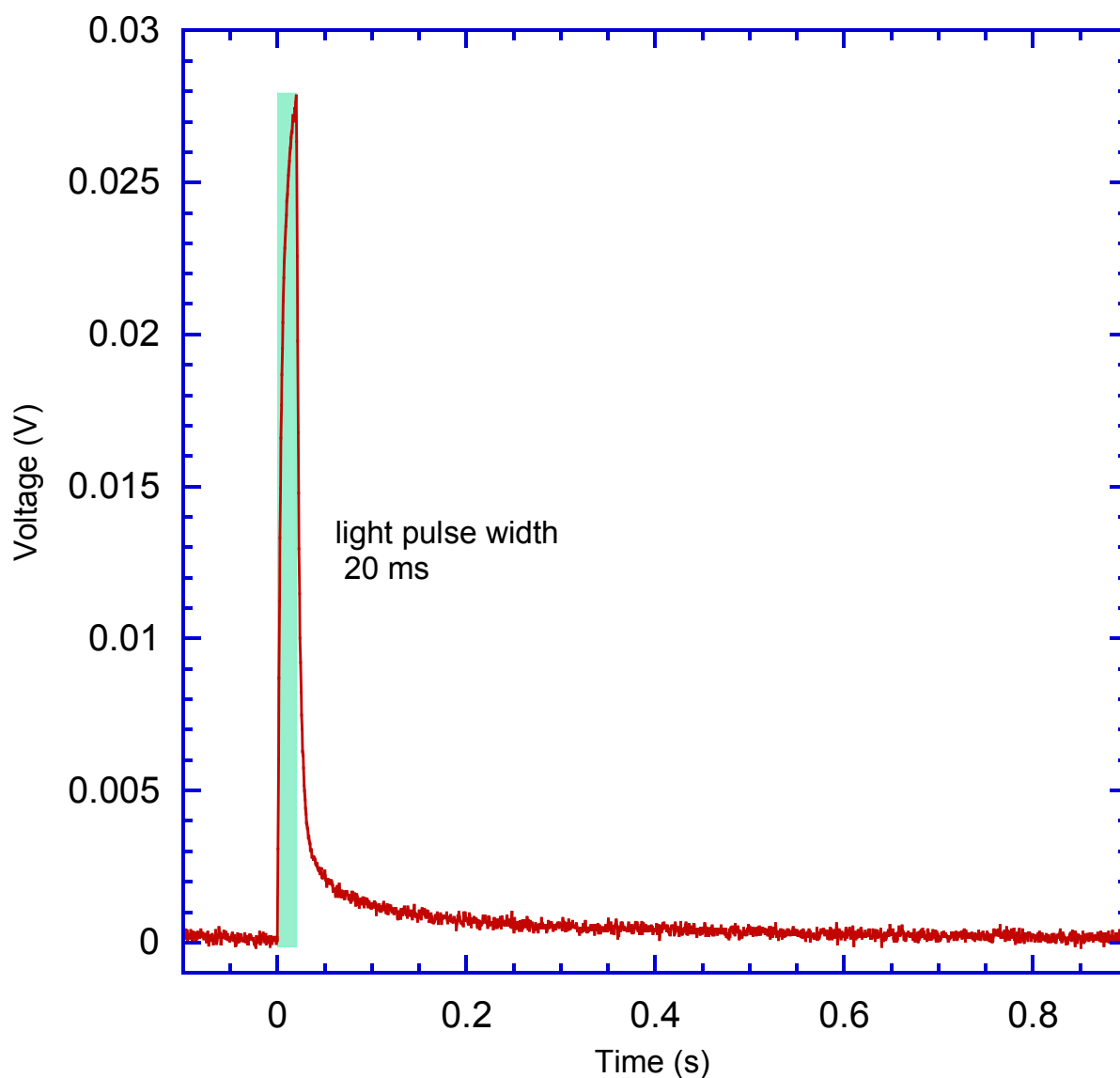


Figure S21. Transient photo-induced current response of thin film, R, N(Ph-2T-DCV-Hex)₃ sample on glass/ITO substrates without ZnO hole blocking interlayer, interfaced with PBS electrolyte obtained with pulsed excitation from 515 nm laser diode. Laser pulse width 20 ms, duty cycle 999 ms. Shaded box illustrates laser pulse width.

References

- 1 O. V. Kozlov, Y. N. Luponosov, A. N. Solodukhin, B. Flament, O. Douhéret, P. Viville, D. Beljonne, R. Lazzaroni, J. Cornil, S. A. Ponomarenko and M. S. Pshenichnikov, *Org. Electron.*, 2018, **53**, 185–190.
- 2 Y.-W. Kao, W.-H. Lee, R.-J. Jeng, C.-F. Huang, J. Y. Wu and R.-H. Lee, *Mater. Chem. Phys.*, 2015, **163**, 138–151.

- 3 Z. Sun, Q. Zang, Q. Luo, C. Lv, F. Cao, Q. Song, R. Zhao, Y. Zhang and W.-Y. Wong, *Chem. Commun.*, 2019, **55**, 4735–4738.
- 4 J. Min, Y. N. Luponosov, D. Baran, S. N. Chvalun, M. A. Shcherbina, A. V. Bakirov, P. V. Dmitryakov, S. M. Peregodova, N. Kausch-Busies, S. A. Ponomarenko, T. Ameri and C. J. Brabec, *J. Mater. Chem. A*, 2014, **2**, 16135–16147.
- 5 S. A. Ponomarenko, S. Kirchmeyer, A. Elschner, N. M. Alpatova, M. Halik, H. Klauk, U. Zschieschang and G. Schmid, *Chem. Mater.*, 2006, **18**, 579–586.
- 6 M. A. Shcherbina, S. N. Chvalun, S. A. Ponomarenko and M. V Kovalchuk, *Russ. Chem. Rev.*, 2014, **83**, 1091–1119.
- 7 N. Sekine, C.-H. Chou, W. L. Kwan and Y. Yang, *Org. Electron.*, 2009, **10**, 1473–1477.
- 8 Tetralin | C₁₀H₁₂ | ChemSpider, <http://www.chemspider.com/Chemical-Structure.8097.html>, (accessed 9 November 2020).